Renewable Energy 224 (2024) 120169

Contents lists available at ScienceDirect

Renewable Energy

journal homepage: www.elsevier.com/locate/renene

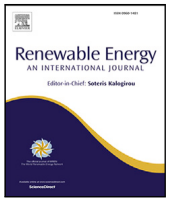

Test Reference Year for wave energy studies: Generation and validation

Francesco Memmola [a,*], Pasquale Contestabile [b,d], Pierpaolo Falco [a,d], Maurizio Brocchini [c]

[a] Università Politecnica delle Marche, Department of Life and Environmental Sciences, Ancona 60131, Italy
[b] Università della Campania "Luigi Vanvitelli", Department of Engineering, 81031 Aversa, Italy
[c] Università Politecnica delle Marche, Department of Civil and Building Engineering and Architecture, Ancona 60131, Italy
[d] Consorzio Nazionale Interuniversitario per le Scienze del Mare (CoNISMa), Roma, P.le Flaminio 9, 00196 Rome, Italy

ARTICLE INFO

Keywords:
Wave energy
Test reference year
ERA-interim
ERA-5
Wave model

ABSTRACT

In a perspective of impoverishment of the fossil fuel and preservation of the natural environment, the sea wave energy is being increasingly regarded as alternative and promising resource. A key aspect to take in consideration for the deployment of Wave Energy Converters is the local characterization of the wave climate. In this contribute, a methodology for the calculation and validation of a site-specific Test Reference Year (TRY), from a multiyear dataset such ERA-Interim and ERA-5, to be used in wave energy conversion studies is proposed. Comparison of the two datasets with observed data gives ERA-5 as the best dataset.

The methodology applied for the TRY generation has proven to be very effective, with the daily sum of H_s and T_m being the most effective indices for the TRY generation and in general H_s about twice more important than T_m. Once obtained, the TRY is applied in order to force an implementation of the Simulating WAves Nearshore (SWAN) model in an area of the central Adriatic Sea to characterize the area.

1. Introduction

The depletion of the fossil fuel and the necessity to preserve the natural environment, is bringing the community interest toward the use of renewable and sustainable energy. In the ocean, one of the most conspicuous and promising forms of energy is the one from ocean waves. One of the main drawbacks of resorting to wave power is its high variability at different time-scales: seasonal and monthly patterns, with the sea state and from wave to wave. Thus, when planning the utilization of wave power, the local characterization of the wave climate is crucial. In the past twenty years, several attempts have been undertaken to map the offshore wave energy and create tools facilitating the computation of nearshore wave energy resources. Global wave energy resource maps have been previously featured in the review book by Cruz [1], utilizing WorldWaves data. Extensive efforts have been dedicated to wave energy assessment along different segments of the European coastline [2–14], in America [15–25], in Africa [26–28], in Asia [29–38] and in Oceania [39–43]. Since adequate wave buoy data are often not available, most of these studies used dataset obtained from meteorological data assimilation, where an atmosphere circulation reanalysis is integrated with a wave model. Therefore, weather forecasts rely on incorporating weather observations collected over decades through a single consistent analysis in forecast models. No wave parameters are assimilated, making the sea surface conditions a hindcast run, where forecasts have always relied on accurate observations of the current weather. Example of reanalysis datasets are the Climate Forecast System Reanalysis and Reforecast provided by the National Oceanic and Atmospheric Administration (NOAA) [44] or the ERA-Interim [45] and ERA-5 [46] provided by the European Centre for Medium-Range Weather Forecasts (ECMWF). While for offshore (deepwater) energetic patterns the wave power assessment is based on simple statistics and calculations of the wave data, i.e. significant wave height (H_s), mean period (T_m) and mean direction (θ_m), nearshore water conditions require preliminary analysis aimed at the propagation of offshore wave climate by means of numerical models. These models, besides requiring accurate calibration activity - possibly based on direct local measurements (e.g. wave buoy, ADCP etc.) [47] – need long computational time [48]. This creates the paradox that even if some decades of wave data are available, in most cases the nearshore propagations are limited to simulate five or ten years. In addition, when power production of a specific wave energy converter (WEC hereinafter) technology is accomplished using multiyear data, more and more expensive computational efforts are required [49], and if wave farms in coastal areas are simulated, prohibitive computational efforts are necessary. The possibility of using a representative sample of the entire dataset has long been strongly advocated by researchers and

* Corresponding author.
E-mail addresses: f.memmola@univpm.it (F. Memmola), pasquale.contestabile@unicampania.it (P. Contestabile), pierpaolo.falco@univpm.it (P. Falco), m.brocchini@univpm.it (M. Brocchini).

https://doi.org/10.1016/j.renene.2024.120169
Received 25 May 2023; Received in revised form 20 January 2024; Accepted 15 February 2024
Available online 19 February 2024

engineers involved in the wave energy sector. An option is to create one year of representative data, usually called "long-term average data series" in the meteorological field [50]. Here, the main shortcoming, is the loss of the data time history and time correlation with the extreme events, due to the aggregation of instantaneous data. Several methodologies exist for the calculation of typical meteorological year, which applies different algorithms and month criteria selection. However, the common feature that all of them share, is the use of real meteorological data to build one single year of data. The seminal work, which inspires mostly all the other methods, is the one proposed by [51] for solar energy systems, which is based on cumulative distribution function; the Danish method makes use of standardized mean square and standardized mean of the residuals ([52,53]); the Festa-Ratto method applies composite distance difference [54]; Petrakis [55] developed a software tool, for the creation of a typical meteorological year, utilizing the Filkenstein–Schafer statistical method [56]; Bilbao et al. proposed a methodology for the generation of a TRY in the Mediterranean area using different methods for the generation [50]; Lee et al. [57] produced TRY for seven major cities from 20 years of meteorological data according to ISO15927 standards; Vestrucci et al. [58] explored the possibility of using an environmental Test Reference Year for modeling in the atmosphere pollutant dispersion. To paraphrase Lund [59], the TRY for WEC assessments shall contain, for all seasons, such a variety of different weather situations that any WEC, regardless of type, orientation, or Power take-off, will get reasonable different excitations to make it possible to get an overall impression of the performance of the device during a typical year. However, to the best of our knowledge, no methodologies have been as yet developed for the construction of a TRY exploitable for WEC studies. Thus, in this effort, by taking the steps from the climatology TRY literature, a preliminary methodology for the calculation of a TRY directly applicable to isolated axisymmetric heaving devices, which are not sensitive to the direction of wave propagation, is proposed. Determined by the prevalent use of TRY for point absorber technologies, the provided algorithm uses as mandatory parameters the significant wave height and the mean wave period, neglecting the wave direction. Once generated, the TRY have been used, for illustrative purposes, to assess the energy resource in a sub region of the central Adriatic Sea characterized by a number of offshore platforms using a numerical approach.

The paper is structured as follows. Section 2 describes the study area and the two datasets used. The methodology for the TRY calculation, the used statistics, the theory for the wave power assessments and the numerical model are described in Section 3. Section 4 contains the wave power resource characterization, with discussions included. Section 5 closes the paper with final considerations.

2. Study area and dataset

The test field is located in the central Adriatic Sea close to the Ortona buoy (see Fig. 1). In general, this coastal area is characterized by fine to very fine-grained sands, extremely gentle slopes and an average depth of 140 m. Here the wave averaged power estimated by [8,60] is about 1.5–2 kW/m.

For the characterization of the wave climate and the construction of the Test Reference Year (TRY), the two datasets ERA-Interim [45] and ERA-5 [46] by the European Centre for Medium-Range Weather Forecasts (ECMWF) where compared, at the virtual station E1 (see Fig. 1), with observed data. The ERA-Interim dataset is a global atmospheric reanalysis archive that contains a variety of parameters, describing weather, land-surface conditions and ocean waves, covering the period from January 1979 to August 2019. The wave model component of ERA-Interim has an horizontal resolution of 1 degree and a wave spectra discretized using 24 directions and 30 frequencies and a 6-hour temporal resolution. Its successor is the ERA-5 reanalysis dataset. Here the wave model component has an horizontal resolution of 0.36 degree and a hourly temporal resolution. The two datasets have been compared with observed data collected by the Italian national data buoy network (RON; [61]), in particular by the Ortona buoy [42.40 N 14.53 E], see Fig. 1.

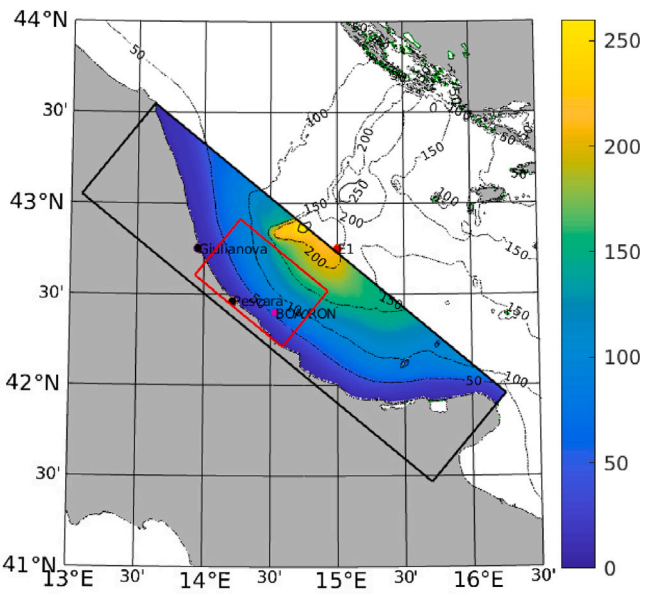

Fig. 1. Study area: SWAN coarse grid (black rectangle), SWAN fine grid (red rectangle), the virtual station E1 (red dot) and the Ortona buoy (magenta dot). The colorbar indicates the depth.

3. Methodology

3.1. Calculation of the average year

The simplest thing one can do to create a year of representative data, is to calculate the average year. That is the hourly specific mean of H_s and T_m for each hour of the year. For the hourly 41 year long dataset ERA-5 used in this study (from January 1979 to December 2019), the 00:00 of the first of January for the ERA-5 average year is given by making the average of all the 41 values of the 00:00 of the first of January.

3.2. Dataset selection

Two statistics, namely the Mean Bias (BIAS) and Root Mean Square Error (RMSE) were used to evaluate the performance of the two multi-year dataset:

$$BIAS = \frac{\sum_{i=1}^{N}(M_{t,i} - M_{ref,i})}{N} \tag{1}$$

$$RMSE = \sqrt{\frac{\sum_{i=1}^{N}(M_{t,i} - M_{ref,i})^2}{N}} \tag{2}$$

where N is the number of time records, M_t is the solution to be tested and M_{ref} is the reference solution.

3.3. The test reference year

3.3.1. Test reference year: the concept

The Typical Meteorological Year (TMY) developed by Sandia National Laboratories in the United States [51,62] is one of the most accepted methods to determine a TRY. It consists of twelve typical meteorological months (TMMs), selected from several calendar months in a multi-year weather dataset. To give an example, the month January 2000 can be selected as the first TMM, the month February 1990 as the second TMM, etc. Once selected, the TMMs are put together to form the TMY. To avoid abrupt changes at the boundary between contiguous months, smoothing is usually required. Thus, the main goal of our contribution is to generate a TRY suitable for wave energy studies,

transferring the methodologies used in the meteorology field to the wave energy subject. Thus, we modified the TMY method in order to build a TRY to be used in the wave energy field.

3.3.2. Test reference year: the method

The selection of the typical month is performed by means of the following three steps.

step 1 The first choice regards the relevant variables for wave energy application. Due to their importance in the calculation of the wave power flux, significant wave height (H_s) and the mean wave period (T_m) are processed. Daily Indices (DI) have been evaluated for the two variables selected. In particular daily minima, maxima, means and sum of both H_s and T_m have been calculated, obtaining a total of eight DI. Then, the cumulative distribution functions (CDFs) have been calculated for each DI on a monthly basis. The CDF is a monotonic increasing, positive definite function with general form:

$$CDF(n) = \sum_{k=1}^{n} P_k \tag{3}$$

where P_k is the relative probability of the discreet variable x_k.

In the following paragraph, a detailed description of the CDF calculation is given. The indices sum of daily H_s (hereinafter SH_s) and the calculation for it of the long-term monthly CDF (42 years in this study) for the month of January is used to portray the method. The method is completely analogous for all other indices and for the short-term monthly CDF (a month of a given year).

Once found the maximum value of SH_s and calculated its integer part ISH_s, the step (STP) is evaluated as:

$$STP = \frac{ISH_s + 1}{30} \tag{4}$$

The bins are defined as: $Bin = k \cdot STP, k = 1, 2, \ldots, 30$ [55], The smallest values of SH_s within each bin are counted and divided by the size of the population, which is $31 \cdot NA$ where 31 is the number of days of January and NA is the number of years in the multi-year database, obtaining the value of the CDF for each bin relative to the month of January.

The cumulative distribution functions (CDFs) for these daily indices are evaluated for each month of the calendar year and are compared to the long-term CDFs using the Finkelstein–Schafer statistics [56],

$$FS_{i,y} = \frac{1}{N} \cdot \sum_{k=1}^{N} \left| CDF_{my}(k) - CDF_{y}(k) \right| \tag{5}$$

where CDF_{my} is the long-term (multy-year) CDF of a given month (e.g January), $CDF_{y,m}$ is the CDF of a given month of a given year (e.g January 1998), the subscript i identifies the considered index, y identifies the year and N is the number of the CDF bin (in this study $N = 31$). Finally a weighted-sum average (WS) of the FS statistic is calculated for each month and the five months with the smallest WS values are selected as candidate month for the final selection (e.g for January the five months of January with the smallest WS values are selected):

$$WS = \frac{1}{m} \sum_{i=1}^{n} WF_i \cdot FS_i \tag{6a}$$

with

$$\sum_{i=1}^{n} WF_i = 1 \tag{6b}$$

where m is the number of DI used and WF_i are the weighting factor for the ith index (see).

step 2 The five selected months are then ranked with respect to:

- the month closeness to the long-term mean and median of H_s and T_m
- the month closeness to the long-term mean of H_s and T_m.

This depending by the performance of the TRY obtained (see Section 4.3). This is accomplished as follows:

- the absolute value of the difference between the long-term mean and median (or just mean) and the mean and median (or just mean) of the five candidates months are calculated for H_s and T_m.
- the calculated differences are than normalized with their maximum difference (e.g., assuming that for the five January months selected the monthly mean differences of H_s are 0.5 m, 0.3 m, 0.2 m, 0.7 m and 0.1 m; then these five values are divided by 0.7 namely, the maximum calculated difference) obtaining for each of the five candidate months 4 (or 2) indices which are added together.
- The month with the smallest sum is selected as the typical month.

step 3 For each calendar month, the best one resulting from step 2 is chosen, and used for the construction of the TRY.

The TRY's performance have been assessed by comparing the hourly mean wave power of each generated TRY and the hourly mean wave power of the whole ERA-5 dataset considered in this work. The weighting factors (WF) have been assessed taking the steps from the pair comparison method [58,63,64]. The procedure is based on the variation of the total yearly wave power (E^y_{tot}; performance indicator) relative to the percentage increment of H_s and T_m (input variables). The first step is to calculate a reference TRY (hereinafter TRY_{ref}) with all weights equal to one, using the procedure explained in Section 3.3.2. The obtained TRY_{ref} is then used for calculation of the reference total yearly wave power $E^{y(ref)}_{tot}$ using Eq. (11). Then, the E^y_{tot} is recalculated increasing separately, for a given number of intervals (e.g. 5%, 10%, etc.), the two input variables allowing, substantially, for the calculation of $\frac{\partial E^y_{tot}}{\partial H_s} \cdot E^{y(ref)-1}_{tot}$ and $\frac{\partial E^y_{tot}}{\partial T_m} \cdot E^{y(ref)-1}_{tot}$. Thus, once retrieved the relative variations for each incremental intervals, they are averaged for each input variables (H_s and T_m). The ratio between the two mean variation allows to quantify the importance of a input variable with respect to the other. The next step is to solve a system of n equations (in this study $n = 2$), where $n - 1$ of them are obtained by equating the ratio of the weights of two variables and the variation of the outputs due to such variables, while the nth equation is obtained by enforcing that the sum of all weights must be equal to one (see Section 4.2 for the application of it).

3.4. Wave power calculation

From the linear theory the total wave energy density (E_t; potential energy plus kinetic energy) is given per unit of horizontal surface area and time averaged over the wave period is

$$E_t = \frac{\rho g H_s^2}{8} \tag{7}$$

where ρ is the sea water density, g is the gravity acceleration and H_s the significant wave height. The energy flux per unit crest length and unit time is

$$P = E_t \cdot C_g \tag{8}$$

in which C_g represents the wave group velocity. In general the mean power theoretical flow P given by:

$$P = \frac{\rho g^2 H_s^2 T_e}{64\pi} \left(\tanh kh + \frac{kh}{\cosh kh^2} \right) \tag{9}$$

in which, according to [14,65], the energy period was assumed as $T_e = 1.14T_m$. In the case of deep water Eq. (9) can be approximated as:

$$P = \frac{\rho g^2}{64\pi} H_s^2 T_e \tag{10}$$

The total wave energy E_{tot} (MW h/m), during a given time interval $\sum_i \partial t_i$ is given by:

$$E_{tot} = \sum_i P_i \partial t_i \tag{11}$$

3.5. Offshore datum propagation

3.5.1. Wave driver

For the present analysis, the offshore datum is propagated onshore using the Simulating WAve Nearshore (SWAN) model within the Coupled Ocean-Atmosphere-Wave-Sediment Transport modeling system framework (COAWST, [66]). SWAN is a phase-averaged, third generation spectral wave model, specifically designed for shallow waters that solves the action balance equation in either stationary or non-stationary mode [67]. The action density, i.e. the wave energy density divided by the relative frequency, is used as the fundamental flow variable because the action density is conserved in the presence of currents. SWAN simulates wind wave generation and propagation in coastal waters and includes the processes of refraction, diffraction, shoaling, wave–wave interactions, and dissipation due to whitecapping, wave breaking, and bottom friction. Specific formulations for wind input, bottom stress, whitecapping, wave–wave interactions, etc. are described in detail in [68].

3.5.2. Model setup

The forcing is provided by the waves incoming perpendicularly to the offshore boundary, while lateral and shoreline boundaries condition are taken as closed. The offshore boundary condition is completed with the generated TRY at the virtual station E1 shown in Fig. 1, which are applied to the whole offshore boundary. The use of closed lateral boundary conditions together with the use of constant waves parameters all along the offshore boundary, can obviously lead to the formation of shadow areas, which may propagate from the grid lateral boundaries. Thus, we use a nesting approach where, within a coarse grid (Fig. 1 black line; with an horizontal resolution of about 1 km) a finer grid (Fig. 1 red line; with an horizontal resolution of about 300 m) is nested. The lateral boundaries of the fine grid have been chosen far enough from the coarse grid's lateral boundaries to be unaffected by the shadow area developed in the coarse grid. The bathymetric data used to compile the computational grids comes from the EMODNET dataset [69].

4. Results

4.1. Offshore datum comparison

The Era-Interim and ERA-5 datasets have been compared between them and with the observed data from the Ortona buoy, when available. Fig. 2 shows the bar chart of the yearly mean for H_s (top panel) and T_m (botom panel) of the three datasets. It is clear that both H_s and T_m are overestimated by using the ERA-Interim dataset when compared with H_s and T_m from the Ortona buoy (see yellow bars in Fig. 2 and positive mean bias in Table 1). However, the virtual station $E1$ is at a depth of about 210 m, while the Ortona buoy lays at a depth of about 60 m. This implies some possible wave energy dissipation of the waves traveling between the two points. Different is the situation when comparing H_s and T_m obtained from the ERA-5 reanalysis (blue bars) and the Ortona buoy, being the two dataset much more similar. However, with some exceptions, the values of H_s and T_m for the ERA-5 dataset (red bars) are slightly underestimated (see Fig. 2 and the negative mean bias in Table 1). The overestimation of the two wave parameters from Era-Interim it is also evident when comparing the monthly mean of H_s and T_m shown in Fig. 3, while the slight underestimation of H_s and T_m from the ERA-5 dataset practically vanishes in the long term means. The monthly means are calculated using all the data available within the time window where the three datasets overlap. In view of our results and of the higher temporal and spatial resolution of the ERA-5 data, we chose ERA-5 as the multi-year dataset to be used for the TRY generation.

Table 1
BIAS and RMSE of H_s and T_m from ERA-Interim and ERA-5 for the period spanning from 01-07-1989 to 18-05-2011.

	H_s		T_m	
Dataset	BIAS	RMSE	BIAS	RMSE
ERA-Interim	0.17455	0.59339	0.70493	1.38375
ERA-5	−0.04590	0.26111	−0.1665	0.80385

Table 2
E_{tot} variations incrementing either H_s or T_m.

Reference E_{tot} (MW h/m)		10384		
H_s increment (%)	5	10	15	20
Produced E_{tot}	11 449	12 566	13 734	14 954
E_{tot} increment (%)	9.3	17.3	24.4	30.6
T_m increment (%)	5	10	15	20
Produced E_{tot}	10 904	11 423	11 942	12 461
E_{tot} increment (%)	4.7	9.1	13.0	16.7
Variation ratio (VH_s/VT_m)	2.0	2.1	2.1	2.2

4.2. Weighting factors calculation

In according with , the $E_{tot}^{y(ref)}$ have been calculate, than E_{tot}^{y} it is calculated increasing separately, H_s and T_m. Table 2 summarizes, the values of the relative variation of E_{tot}^{y} due to the increment of H_s and T_m. The mean value of the ratio among variations $\overline{VH_s/VT_m}$ (V stand for variation and overline is used to indicates the mean) is 2.125, which means that H_s is about twice more important than T_m. Equating the ratio of the weights of the two input variables (H_s and T_m) and the variation of the outputs (E_{tot}^{y}) and enforcing that the sum of all weights must be equal to one, the weighting factors are given by:

$$\begin{cases} (n-1),\ W_H - 2.125W_T = 0 \\ (n^{th}),\ W_H + W_T = 1 \end{cases} \tag{12a}$$

which yields:

$$\begin{cases} W_H = 0.68 \\ W_T = 0.32 \end{cases} \tag{12b}$$

4.3. Test reference year: selection

Using the methodology introduced in Section 3.3 and different combinations of indices, such as H_s daily mean, daily sum and so on, we built and tested several TRYs. All the TRYs built using both monthly mean and median of H_s and T_m after the application of the FS statistic (namely during the step 2 described in Section 3.3.2), had a worse performance compared with their counterpart selected only using the monthly mean and, thus, are not considered in this work. The assessment of the devised TRYs has been accomplished by comparing the hourly mean wave power obtained by each TRY, with that calculated from the whole ERA-5 dataset (reference solution). Table 3 summarize, the reference solution, the hourly mean wave power calculated from each TRY and the hourly mean wave power calculated by the average (hourly based) year obtained from the ERA-5 dataset.

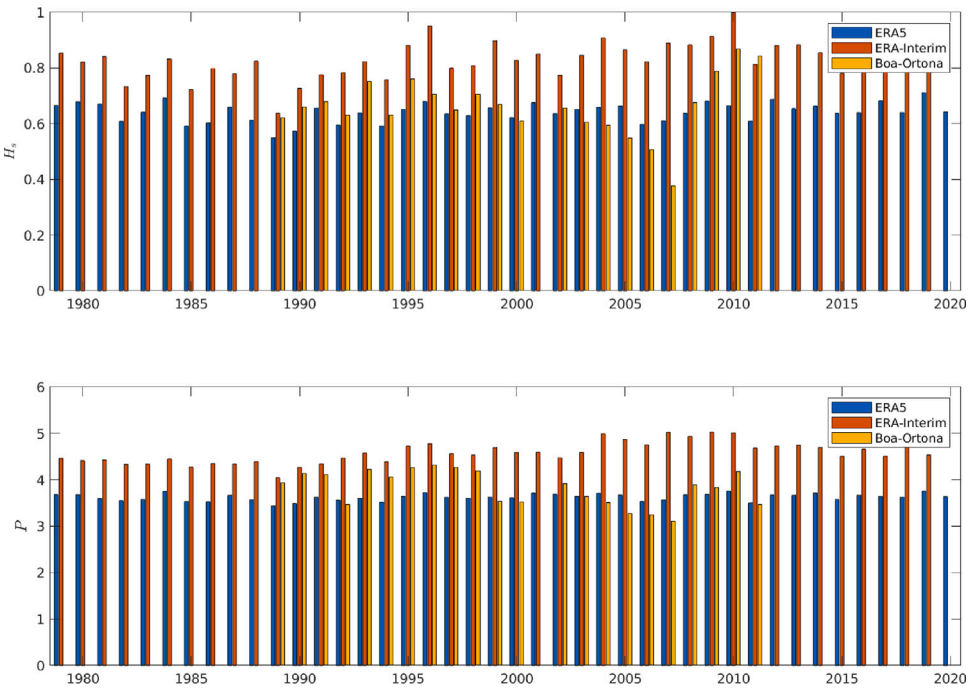

Fig. 2. Yearly mean of H_s top panel and T_m bottom panel of ERA-Interim, ERA-5 and the observed data from the RON buoy.

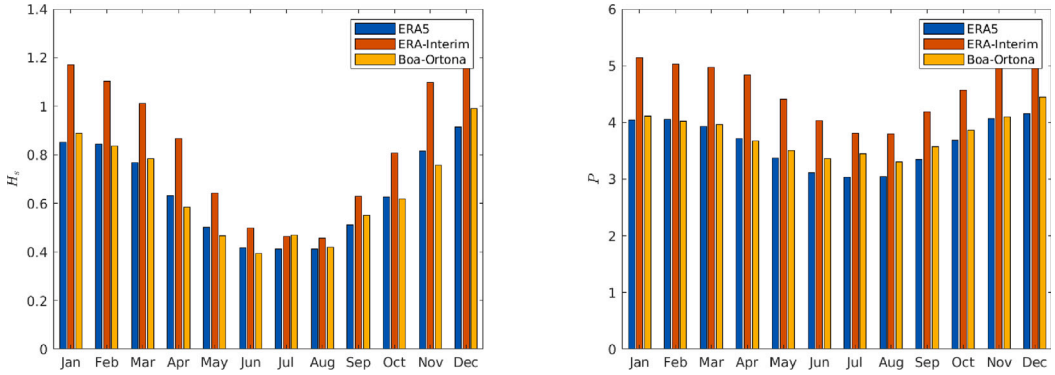

Fig. 3. Monthly mean of H_s (top panel) and T_m (bottom panel) of ERA-Interim, ERA-5 and the observed data from the RON buoy.

Table 3
Hourly mean wave power of the generate TRYs, reference solution and ERA-5 averaged year. The indices names min, max, mean and sum are intended as the daily min, max, mean and sum of both: H_s and T_m.

TRY name	Indices in use	Hourly mean wave power (kW/m)
TRY1	min, max, mean, sum	1.607
TRY2	min, max, mean	1.537
TRY3	min, max, sum	1.808
TRY4	min, mean	1.537
TRY5	max, mean	0.746
TRY6	min, sum	1.230
TRY7	max, sum	1.754
TRY8	mean, sum	**1.827**
TRY9	mean	0.871
TRY10	sum	1.377
Reference solution	–	1.839
ERA-5 average year	–	0.807

The different TRYs have been generated using different combination of the indices such as daily minima, daily maxima, daily means and daily sum of both H_s and T. Table 3 allows one to identify the phenomenon (but not its underlying mechanism) for which the mean wave power obtained from the average year is completely different from the one computed using the same, whole dataset: implications for WEC design could be disastrous. To understand the related underlying causes it is crucial to highlight the interannual variability in a climate system. Low-frequency anomalies in weather conditions appear to have a significant impact on the average year. Therefore, existence of large-scale coherent patterns of multiyear variability in storm/calm wave

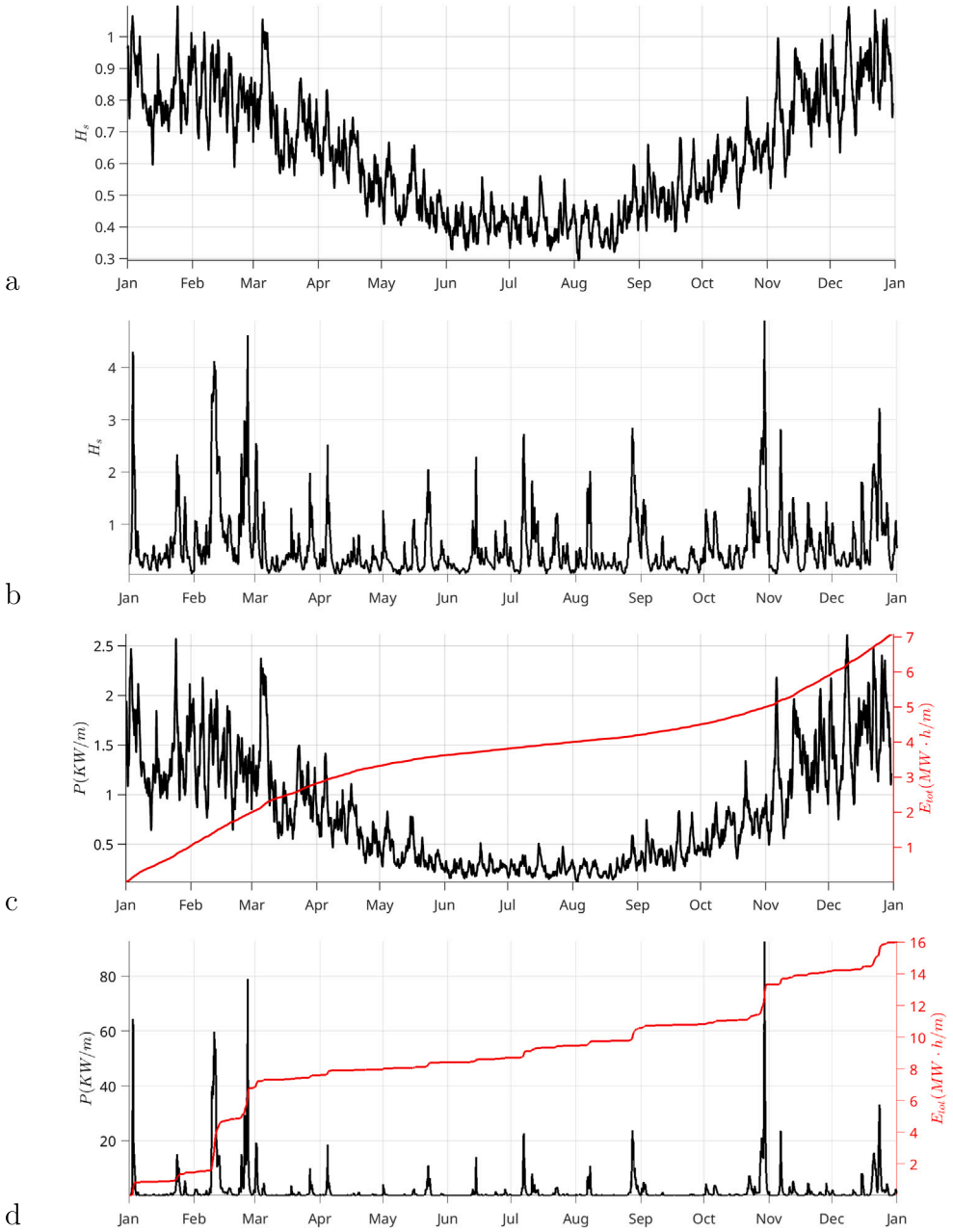

Fig. 4. Time series of significant wave height H_s: ERA-5 average year (a), TRY8 (b). Time series of wave power P: ERA-5 average year (c), TRY8 (d). Panels (c) and (d) also give (red line) the total potentially produced energy E_{tot}.

conditions in a site, provides ample evidence for an objective impossibility to obtain robust and representative information about the wave climate using the simple approach of the average year. The TRY here generated shows very good performance in providing a representative yearly mean power level. Our results highlight that the most important index for the generation of a suitable TRY from a multi-year dataset are the daily sum of H_s and T_m. In fact, the TRYs obtained by these two indices, with the exception of TRY6, have their hourly wave power closer to the reference solution (see Table 3). However, the best result is obtained when using as reference indices both the daily mean and the daily sum of H_s and T_m (TRY8, see Table 3). H_s, the estimated P and E_{tot} obtained for TRY8 and for the ERA-5 average year using Eqs. (10) and (11) respectively, are shown in Fig. 4. The ERA-5 average year completely fails in representing the extreme, with a maximum H_s slightly above 1 m (Fig. 4 a). This value is about 4 times smaller than the maximum H_s of the TRY8 (Fig. 4 b). The maximum wave power calculated from TRY8 is higher than 80 kW/m, which is a value comparable with other areas of the Adriatic sea [70] and about 32 times higher of the one calculated from the ERA-5 average year (see Fig. 4).

4.4. Numerical model data

Numerical model data have been used to assess the energy content in each computational cell of the study area. The wave parameters H_s and T_m computed by SWAN have been used to estimate the total wave energy (E_{tot}) integrating Eq. (11) for the whole year and the results are shown in Fig. 5. While Fig. 6 gives the percentage of E_{tot} decrease. Starting from the offshore boundary of the coarse grid (Fig. 5, top panel) and going toward the offshore boundary of the fine grid, the total energy E_{tot} during the whole TRY decays pretty fast, regardless of the depth. Then, at about 10 km from the offshore boundary, the decay of E_{tot} slows down dramatically and once into the fine grid domain

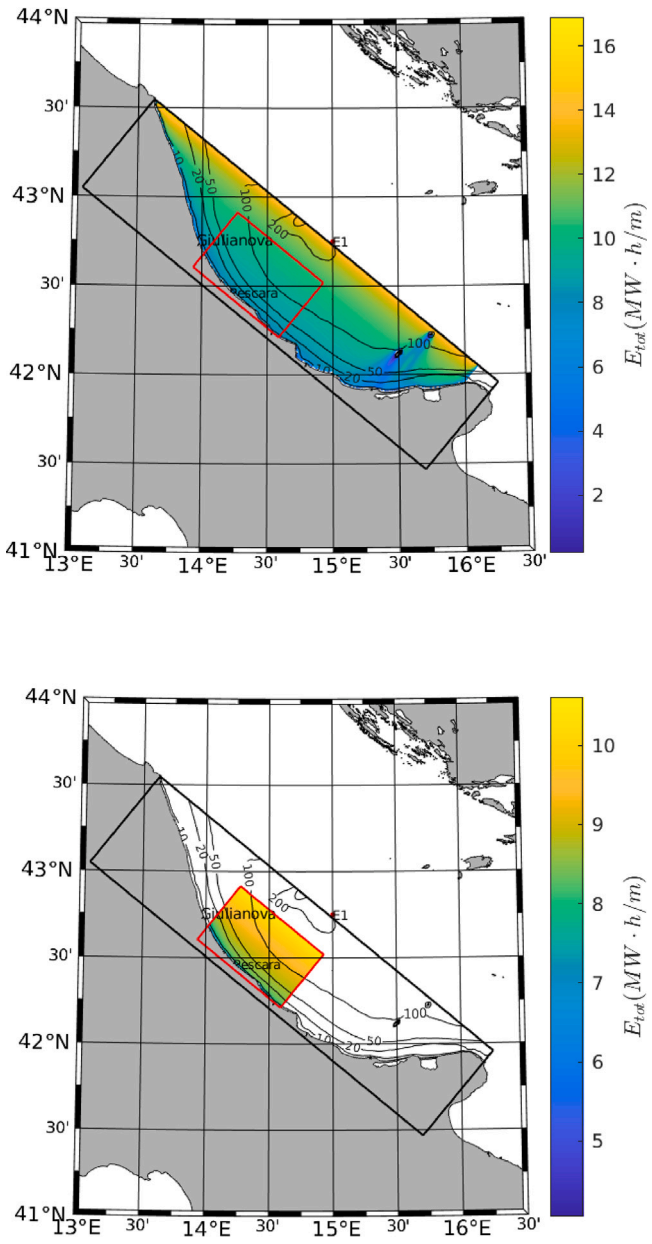

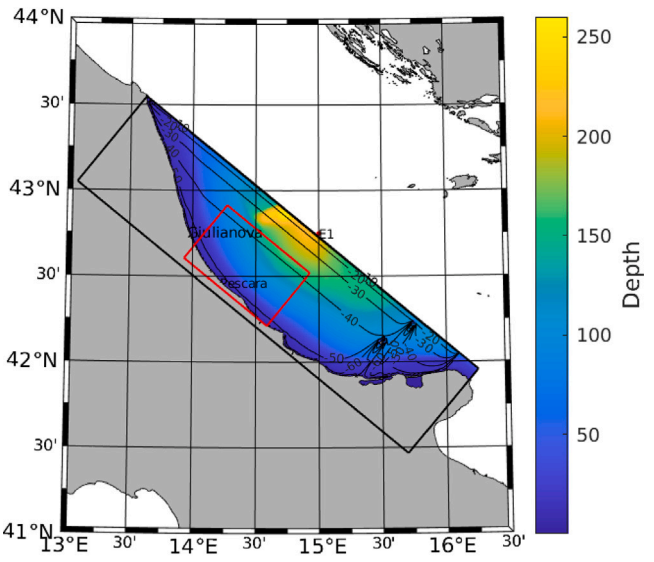

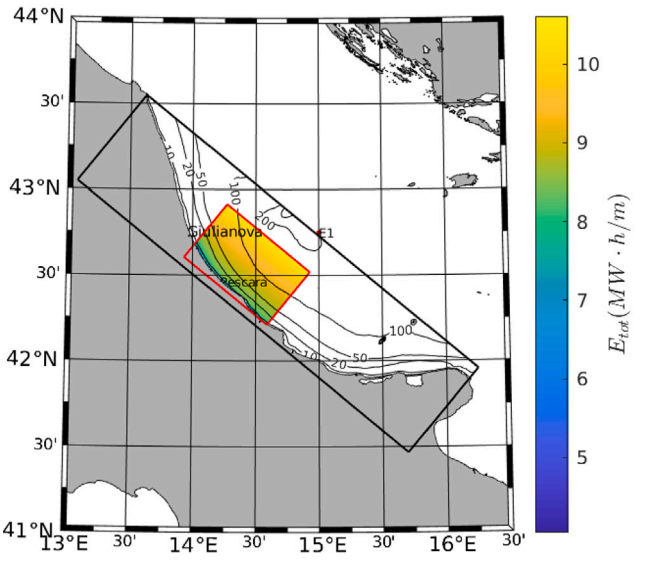

Fig. 5. Total wave energy E_{tot} (colormap). The bathymetry (isolines). Coarse grid (top panel) and fine grid (bottom panel).

Fig. 6. Percentage of total wave energy E_{tot} loss or gain with respect to the corresponding value of E_{tot} at the offshore boundary of the coarse grid (isolines) and bathymetry (colormap). Coarse grid (top panel) and fine grid (bottom panel).

(Fig. 5, bottom panel) the loss of E_{tot} becomes very slow till the 50 m bathymetric, where the wave energy likely starts to decay because of wave breaking (see Fig. 5). The amount of energy loss is quantified in Fig. 6 where the contour lines represent the percentage of energy lost with respect to the corresponding value of at the offshore boundary of the coarse grid, while the colormap represents the depth. The top panel of Fig. 6 shows that moving from the offshore boundary toward the coast E_{tot} decreases fast till the lost of the 30% of energy when the wave are still in deep water (see Fig. 6). Moving further to shore, the energy loss slows down till reaching the contour that indicates the 40% of energy loss. Then, the E_{tot} decrease become even smaller, reaching the contour where 50% of energy is lost very close to the coast (see Fig. 6). These results suggest that there is a large amount of wave energy dissipated in deep waters. This is likely due to the white-capping phenomenon.

5. Discussion and conclusions

The main goal of the present study was to propose an innovative, preliminary methodology for the generation of a test reference year suitable for wave energy analyses and to evaluate energy production from WECs using hydrodynamic modeling software. Within our study, the differences between the TRY and the average year were highlighted. The results suggest that use of long-term average data series (the ERA-5 average year in Table 3) for wave energy studies can lead to incorrect conclusions. The algorithm here provided focuses on significant wave height and mean wave period, which could be properly used to assess the potential wave energy striking a stand-alone axisymmetric heaving/oscillating device, as well as point absorbers. Future works will focus on the inclusion of the wave direction. The two reanalysis datasets Era-Interim and ERA-5 have been compared, in order to select the multiyear dataset to be used for the TRY generation.

Once generated the TRY, the same was used to complete the off - shore boundary condition for a numerical simulation, run with SWAN, to study the energy resource available in a sub region of the central Adriatic Sea characterized by a number of offshore platforms and where point absorber type WECs were shown to be one of the best solutions [71].

Comparison of the two datasets with observed data coming from the Ortona wave buoy gives ERA-5 as the best dataset, showing 1.84 kW/m against the 1.90 kW/m from the direct measurements.

The methodology applied for the TRY generation has proven to be very effective, at least for the cases under analysis. The daily sum of H_s and T_m are seen to be the most effective indices for a TRY generation, with the best results achieved when using as indices both the daily mean and the daily sum of H_s and T_m (see TRY8 in Table 3). However, the analyses here performed are not extensive enough to definitively suggest a combination of indices to be used. Thus, we suggest further studies are performed to assess different combinations of the proposed indices to generate the best possible TRY. Further, our results suggest that use of long-term average data series (the ERA-5 average year in Table 3) for wave energy studies can lead to incorrect conclusions. The results of the numerical simulations suggest that there is a considerable loss of energy when transferring the wave field from the offshore toward the coast as expected. A conspicuous amount of this energy dissipation occurs when the waves are still in deep waters, this suggesting the white-capping as possible dissipation mechanism. TRY is integral to strategic environmental and feasibility assessment of WEC farms and to assess the performance of devices at design stage, enabling representative but faster and more stable numerical calculations. The algorithm here proposed could lead to a major advancement of current understanding of climate variability, setting the stage for innovative predictability systems.

CRediT authorship contribution statement

Francesco Memmola: Conceptualization, Data curation, Formal analysis, Methodology, Software, Writing – original draft, Writing – review & editing. **Pasquale Contestabile:** Conceptualization, Writing – original draft, Writing – review & editing. **Pierpaolo Falco:** Supervision, Writing – original draft, Formal analysis, Writing – review & editing. **Maurizio Brocchini:** Funding acquisition, Supervision, Writing – original draft, Writing – review & editing.

Declaration of competing interest

The authors declare that they have no known competing financial interests or personal relationships that could have appeared to influence the work reported in this paper.

Acknowledgments

Financial support from the Italian PlaCE Project (code ARS01_00891), a National Research Programme funded by the Italian Ministry of University and Research through "PON R&I 2014–2020 e FSC" funds, are gratefully acknowledged.

References

[1] J. Cruz, Ocean Wave Energy: Current Status and Future Prespectives, Springer Science & Business Media, 2007.
[2] K. Nielsen, N.I. Meyer, The danish wave energy programme, in: Proceedings of the 3rd European Wave Energy Conference, Vol. 30, Patras, Greece, 1998.
[3] M.T. Pontes, R. Aguiar, H. Oliveira Pires, A nearshore wave energy atlas for Portugal, 2005.
[4] G. Iglesias, R. Carballo, Wave energy potential along the Death Coast (Spain), Energy 34 (11) (2009) 1963–1975.
[5] R. Waters, J. Engström, J. Isberg, M. Leijon, Wave climate off the Swedish west coast, Renew. Energy 34 (6) (2009) 1600–1606.
[6] G. Iglesias, R. Carballo, Wave energy resource in the Estaca de Bares area (Spain), Renew. Energy 35 (7) (2010) 1574–1584.
[7] G. Iglesias, R. Carballo, Wave resource in El Hierro—An island towards energy self-sufficiency, Renew. Energy 36 (2) (2011) 689–698.
[8] D. Vicinanza, L. Cappietti, V. Ferrante, P. Contestabile, Estimation of the wave energy in the Italian offshore, J. Coast. Res. (2011) 613–617.
[9] D. Vicinanza, P. Contestabile, V. Ferrante, Wave energy potential in the north-west of Sardinia (Italy), Renew. Energy 50 (2013) 506–521.
[10] S.P. Neill, M.J. Lewis, M.R. Hashemi, E. Slater, J. Lawrence, S.A. Spall, Inter-annual and inter-seasonal variability of the Orkney wave power resource, Appl. Energy 132 (2014) 339–348.
[11] C. Iuppa, L. Cavallaro, D. Vicinanza, E. Foti, Investigation of suitable sites for wave energy converters around Sicily (Italy), Ocean Sci. 11 (4) (2015) 543–557.
[12] V. Venugopal, R. Nemalidinne, Wave resource assessment for scottish waters using a large scale North Atlantic spectral wave model, Renew. Energy 76 (2015) 503–525.
[13] N. Jadidoleslam, M. Özger, N. Ağıralioğlu, Wave power potential assessment of Aegean Sea with an integrated 15-year data, Renew. Energy 86 (2016) 1045–1059.
[14] P. Contestabile, S. Russo, A. Azzellino, F. Cascetta, D. Vicinanza, Combination of local sea winds/land breezes and nearshore wave energy resource: Case study at MaRELab (Naples, Italy), Energy Convers. Manage. 257 (2022) 115356.
[15] N. Lanfredi, J. Pousa, C. Mazio, W. Dragani, Wave-power potential along the coast of the province of Buenos Aires, Argentina, Energy 17 (11) (1992) 997–1006.
[16] G. Hagerman, Southern New England wave energy resource potential, in: Proceedings of the Building Energy, Tufts University Boston, MA, USA, 2001.
[17] A. Cornett, Ventory of Canada's marine renewable nergy resources, 2006.
[18] J.H. Wilson, A. Beyene, California wave energy resource evaluation, in: International Conference on Offshore Mechanics and Arctic Engineering, Vol. 42711, 2007, pp. 549–562.
[19] Z. Defne, K.A. Haas, H.M. Fritz, Wave power potential along the Atlantic coast of the southeastern USA, Renew. Energy 34 (10) (2009) 2197–2205.
[20] D. Dunnett, J.S. Wallace, Electricity generation from wave power in Canada, Renew. Energy 34 (1) (2009) 179–195.
[21] P. Lenee-Bluhm, R. Paasch, H.T. Özkan-Haller, Characterizing the wave energy resource of the US Pacific Northwest, Renew. Energy 36 (8) (2011) 2106–2119.
[22] J.E. Stopa, K.F. Cheung, Y.-L. Chen, Assessment of wave energy resources in Hawaii, Renew. Energy 36 (2) (2011) 554–567.
[23] B.R. Robertson, C.E. Hiles, B.J. Buckham, Characterizing the near shore wave energy resource on the west coast of Vancouver Island, Canada, Renew. Energy 71 (2014) 665–678.
[24] P. Contestabile, V. Ferrante, D. Vicinanza, Wave energy resource along the coast of Santa Catarina (Brazil), Energies 8 (12) (2015) 14219–14243.
[25] A. Mariani, G. Crispino, P. Contestabile, F. Cascetta, C. Gisonni, D. Vicinanza, A. Unich, Optimization of low head axial-flow turbines for an overtopping breakwater for energy conversion: A case study, Energies 14 (15) (2021) 4618.
[26] P. Contestabile, D. Vicinanza, Coastal defence integrating wave-energy-based desalination: A case study in madagascar, J. Mar. Sci. Eng. 6 (2) (2018) 64.
[27] C. Fourie, D. Johnson, The wave power potential of South Africa, Power-Gen Africa (2017).
[28] O. Kayode, O. Koya, Wave energy potential along the Gulf of Guinea coast of Nigeria, Appl. Eng. Lett. 4 (4) (2019).
[29] F. Chen, S.-M. Lu, K.-T. Tseng, S.-C. Lee, E. Wang, Assessment of renewable energy reserves in Taiwan, Renew. Sustain. Energy Rev. 14 (9) (2010) 2511–2528.
[30] G. Kim, W.M. Jeong, K.S. Lee, K. Jun, M.E. Lee, Offshore and nearshore wave energy assessment around the Korean Peninsula, Energy 36 (3) (2011) 1460–1469.
[31] C. Zheng, J. Xu, C. Zhan, Q. Wang, 21st Century Maritime Silk Road: Wave Energy Resource Evaluation, Springer, 2020.
[32] C.W. Zheng, C.Y. Li, Variation of the wave energy and significant wave height in the China Sea and adjacent waters, Renew. Sustain. Energy Rev. 43 (2015) 381–387.
[33] Y. Wan, J. Zhang, J. Meng, J. Wang, Exploitable wave energy assessment based on ERA-Interim reanalysis data—A case study in the East China Sea and the South China Sea, Acta Oceanol. Sinica 34 (2015) 143–155.
[34] B. Aydoğan, B. Ayat, Y. Yüksel, Black sea wave energy atlas from 13 years hindcasted wave data, Renew. Energy 57 (2013) 436–447.
[35] D.K. Ly, V.M. Aboobacker, S. Abundo, N. Srikanth, P. Tralich, Wave energy resource assessment for southeast Asia, in: Proceedings of the 5th International Conference on Sustainable Energy and Environment (SEE), Science, Technology and Innovation for Association of Southeast Asian Nations, ASEAN Green Growth, Bangkok, Thailand, 2014, pp. 19–21.
[36] V.S. Kumar, T. Anoop, Wave energy resource assessment for the Indian shelf seas, Renew. Energy 76 (2015) 212–219.
[37] P. Contestabile, E. Di Lauro, P. Galli, C. Corselli, D. Vicinanza, Offshore wind and wave energy assessment around Malè and Magoodhoo Island (Maldives), Sustainability 9 (4) (2017) 613.

[38] M. Sağlam, E. Sulukan, T.S. Uyar, Wave energy and technical potential of Turkey, J. Nav. Sci. Eng. 6 (2) (2010) 34–50.
[39] M.G. Hughes, A.D. Heap, National-scale wave energy resource assessment for Australia, Renew. Energy 35 (8) (2010) 1783–1791.
[40] M. Hemer, D. Griffin, The wave energy resource along Australia's Southern margin, J. Renew. Sustain. Energy 2 (4) (2010).
[41] S. Behrens, J. Hayward, M. Hemer, P. Osman, Assessing the wave energy converter potential for Australian coastal regions, Renew. Energy 43 (2012) 210–217.
[42] P. Contestabile, E. Di Lauro, M. Buccino, D. Vicinanza, Economic assessment of overtopping breakwater for energy conversion (OBREC): a case study in Western Australia, Sustainability 9 (1) (2016) 51.
[43] J. Morim, N. Cartwright, A. Etemad-Shahidi, D. Strauss, M. Hemer, Wave energy resource assessment along the Southeast coast of Australia on the basis of a 31-year hindcast, Appl. Energy 184 (2016) 276–297.
[44] National Oceanic and Atmospheric Administration, URL https://polar.ncep.noaa.gov/waves/hindcasts/nopp-phase2.php.
[45] D.P. Dee, S.M. Uppala, A. Simmons, P. Berrisford, P. Poli, S. Kobayashi, U. Andrae, M. Balmaseda, G. Balsamo, d.P. Bauer, et al., The ERA-interim reanalysis: Configuration and performance of the data assimilation system, Q. J. R. Meteorol. Soc. 137 (656) (2011) 553–597.
[46] H. Hersbach, B. Bell, P. Berrisford, S. Hirahara, A. Horányi, J. Muñoz-Sabater, J. Nicolas, C. Peubey, R. Radu, D. Schepers, A. Simmons, C. Soci, S. Abdalla, X. Abellan, G. Balsamo, P. Bechtold, G. Biavati, J. Bidlot, M. Bonavita, G. De Chiara, P. Dahlgren, D. Dee, M. Diamantakis, R. Dragani, J. Flemming, R. Forbes, M. Fuentes, A. Geer, L. Haimberger, S. Healy, R.J. Hogan, E. Hólm, M. Janisková, S. Keeley, P. Laloyaux, P. Lopez, C. Lupu, G. Radnoti, P. de Rosnay, I. Rozum, F. Vamborg, S. Villaume, J.-N. Thépaut, The ERA5 global reanalysis, Q. J. R. Meteorol. Soc. 146 (730) (2020) 1999–2049, http://dx.doi.org/10.1002/qj.3803, arXiv:https://rmets.onlinelibrary.wiley.com/doi/pdf/10.1002/qj.3803, URL https://rmets.onlinelibrary.wiley.com/doi/abs/10.1002/qj.3803.
[47] F. Dentale, P. Furcolo, E. Pugliese Carratelli, F. Reale, P. Contestabile, G.R. Tomasicchio, Extreme wave analysis by integrating model and wave buoy data, Water 10 (4) (2018) 373.
[48] P. Contestabile, F. Conversano, L. Centurioni, U.M. Golia, L. Musco, R. Danovaro, D. Vicinanza, Multi-collocation-based estimation of wave climate in a non-tidal bay: The case study of Bagnoli-Coroglio bay (tyrrhenian sea), Water 12 (7) (2020) 1936.
[49] G. Palma, S. Mizar Formentin, B. Zanuttigh, P. Contestabile, D. Vicinanza, Numerical simulations of the hydraulic performance of a breakwater-integrated overtopping wave energy converter, J. Mar. Sci. Eng. 7 (2) (2019) 38.
[50] J. Bilbao, A. Miguel, J. Franco, A. Ayuso, Test reference year generation and evaluation methods in the continental Mediterranean area, J. Appl. Meteorol. Climatol. 43 (2) (2004) 390–400.
[51] I.J. Hall, R.R. Prairie, H.E. Anderson, E.C. Boes, Generation of a typical meteorological year, URL https://www.osti.gov/biblio/7013202.
[52] B. Andersen, S. Eidorff, H. Lund, E. Pedersen, S. Rosenorn, O. Valbjorn, Meteorological Data for Design of Building and Installation: A Reference Year, An English Translation of the Danish Building Research Report 89, 1977.
[53] H. Lund, S. Eidorff, Selection method for production of test reference years, Final Report, Short Version, 1981.
[54] R. Festa, C.F. Ratto, Proposal of a numerical procedure to select reference years, Sol. Energy 50 (1) (1993) 9–17.
[55] M. Petrakis, S. Lykoudis, P. Kassomenos, A software tool for the creation of a typical meteorological year, Environ. Softw. 11 (4) (1996) 221–227.
[56] J.M. Finkelstein, R.E. Schafer, Improved goodness-of-fit tests, Biometrika 58 (3) (1971) 641–645.
[57] K. Lee, H. Yoo, G.J. Levermore, Generation of typical weather data using the ISO Test Reference Year (TRY) method for major cities of South Korea, Build. Environ. 45 (4) (2010) 956–963.
[58] P. Vestrucci, A test reference year (TRY) approach to gas dispersion in the atmosphere, Int. J. Environ. Pollut. 43 (4) (2010) 287–307.
[59] H. Lund, "Test Reference Year", Weather Data for Environmental Engineering and Energy Consumption in Buildings, Thermal Insulation Laboratory, Technical University of Denmark Lyngby, Denmark, 1975.
[60] L. Liberti, A. Carillo, G. Sannino, Wave energy resource assessment in the Mediterranean, the Italian perspective, Renew. Energy 50 (2013) 938–949.
[61] M. Bencivenga, G. Nardone, F. Ruggiero, D. Calore, The Italian data buoy network (RON), Adv. Fluid Mech. IX 74 (321) (2012) 305.
[62] W. Marion, K. Urban, User's Manual for TMY2s (Typical Meteorological Years)-Derived from the 1961–1990 National Solar Radiation Data Base, Tech. Rep., National Renewable Energy Lab.(NREL), Golden, CO (United States), 1995.
[63] K.D. Song, Building Orientation and Local Climatic Conditions (Ph.D. thesis), University of Oklahoma, 1989.
[64] P.R. Drake, Using the analytic hierarchy process in engineering education, Int. J. Eng. Educ. 14 (3) (1998) 191–196.
[65] Atlas of UK Marine Renewable Energy Resources: Technical Report; Report No. R.1106 Prepared for the UK Department of Trade and Industry, Tech. Rep.
[66] J.C. Warner, B. Armstrong, R. He, J.B. Zambon, Development of a Coupled Ocean-Atmosphere-Wave-Sediment Transport (COAWST) Modeling System, Ocean Model. 35 (3) (2010) 230–244, http://dx.doi.org/10.1016/j.ocemod.2010.07.010.
[67] L.H. Holthuijsen, Waves in Oceanic and Coastal Waters, Cambridge University Press, 2010.
[68] N. Booij, I. Haagsma, L.H. Holthuijsen, A. Kieftenburg, R. Ris, A. van der Westhuysen, M. Ziljlema, SWAN Cycle III version 40.41 User Manual, Delft University of Technology, 2004.
[69] S. Thierry, S. Dick, S. George, L. Benoit, P. Cyrille, EMODnet Bathymetry a compilation of bathymetric data in the European waters, in: OCEANS 2019-Marseille, IEEE, 2019, pp. 1–7.
[70] F. Barbariol, A. Benetazzo, S. Carniel, M. Sclavo, Improving the assessment of wave energy resources by means of coupled wave-ocean numerical modeling, Renew. Energy 60 (2013) 462–471.
[71] E. Dallavalle, B. Zanuttigh, P. Contestabile, A. Giuggioli, D. Speranza, Improved methodology for the optimal mixing of renewable energy sources and application to a multi-use offshore platform, Renew. Energy 210 (2023) 575–590.